A PIP1 Aquaporin Contributes to Hydrostatic Pressure-Induced Water Transport in Both the Root and Rosette of Arabidopsis[1[C][W]]

Olivier Postaire[2,3], Colette Tournaire-Roux[2], Alexandre Grondin, Yann Boursiac, Raphaël Morillon, Anton R. Schäffner, and Christophe Maurel*

Biochimie et Physiologie Moléculaire des Plantes, Institut de Biologie Intégrative des Plantes, UMR 5004 CNRS/UMR 0386 INRA/Montpellier SupAgro/Université Montpellier 2, F–34060 Montpellier cedex 1, France (O.P., C.T.-R., A.G., Y.B., C.M.); Amélioration Génétique des Espèces à Multiplication Végétative, Unité Propre de Recherche CIRAD, Instituto Valenciano de Investigaciones Agrarias, 46113 Moncada, Valencia, Spain (R.M.); and Institute of Biochemical Plant Pathology, Helmholtz Zentrum München, German Research Center for Environmental Health, 85764 Neuherberg, Germany (A.R.S.)

Aquaporins are channel proteins that facilitate the transport of water across plant cell membranes. In this work, we used a combination of pharmacological and reverse genetic approaches to investigate the overall significance of aquaporins for tissue water conductivity in Arabidopsis (*Arabidopsis thaliana*). We addressed the function in roots and leaves of AtPIP1;2, one of the most abundantly expressed isoforms of the plasma membrane intrinsic protein family. At variance with the water transport phenotype previously described in AtPIP2;2 knockout mutants, disruption of AtPIP1;2 reduced by 20% to 30% the root hydrostatic hydraulic conductivity but did not modify osmotic root water transport. These results document qualitatively distinct functions of different PIP isoforms in root water uptake. The hydraulic conductivity of excised rosettes (K_{ros}) was measured by a novel pressure chamber technique. Exposure of Arabidopsis plants to darkness increased K_{ros} by up to 90%. Mercury and azide, two aquaporin inhibitors with distinct modes of action, were able to induce similar inhibition of K_{ros} by approximately 13% and approximately 25% in rosettes from plants grown in the light or under prolonged (11–18 h) darkness, respectively. Prolonged darkness enhanced the transcript abundance of several *PIP* genes, including *AtPIP1;2*. Mutant analysis showed that, under prolonged darkness conditions, AtPIP1;2 can contribute to up to approximately 20% of K_{ros} and to the osmotic water permeability of isolated mesophyll protoplasts. Therefore, AtPIP1;2 can account for a significant portion of aquaporin-mediated leaf water transport. The overall work shows that AtPIP1;2 represents a key component of whole-plant hydraulics.

The plant water status is constantly challenged by diurnal variations in environmental parameters, such as light and temperature, or sustained changes in soil water availability or atmospheric humidity. On the long term, plants respond by adjustments of their hydraulic architecture, mostly through altered root and shoot growth and differentiation. On the short term, plant responses rely on stomatal regulation together with rapid changes in hydraulic conductivities of the root (Lp_r) and the leaf (K_{leaf}).

The hydraulic conductance of living tissues integrates the contribution of parallel paths for water transport, across cell walls (apoplastic path) or from cell-to-cell through plasmodesmata (symplastic path) or membranes (transcellular path). The respective contribution of these paths has been mainly addressed in the context of root water uptake (Steudle and Peterson, 1998). In complement to biophysical analyses, several recent studies have provided strong pharmacological and genetic evidence for an overall role of membranes and water channel proteins (aquaporins) in roots (Maggio and Joly, 1995; Siefritz et al., 2002; Javot et al., 2003; Tournaire-Roux et al., 2003). A comprehensive understanding of how distinct cell layers and individual aquaporin isoforms contribute to the overall water transport capacity of the root and to its dynamic regulation is still being developed (Javot et al., 2003; Bramley et al., 2009). Similar questions have arisen in recent studies addressing the paths that mediate the transport of liquid water in inner leaf tissues, from the veins to the stomatal

[1] This work was supported in part by a grant from the French Ministry of Research (ACI2003 "Biologie du Développement et Physiologie Intégrative"), by the Agence Nationale de la Recherche (ANR–05–GPLA–034–06 and ANR–07–BLAN–0226), and by the Deutsche Forschungsgemeinschaft (SPP1108, Scha 454/8).

[2] These authors contributed equally to the article.

[3] Present address: UMR INRA/USTL, Estrées-Mons BP 50136, F–80203 Peronne, France.

* Corresponding author; e-mail maurel@supagro.inra.fr.

The author responsible for distribution of materials integral to the findings presented in this article in accordance with the policy described in the Instructions for Authors (www.plantphysiol.org) is: Christophe Maurel (maurel@supagro.inra.fr).

[C] Some figures in this article are displayed in color online but in black and white in the print edition.

[W] The online version of this article contains Web-only data.

www.plantphysiol.org/cgi/doi/10.1104/pp.109.145326

chamber (Sack and Holbrook, 2006; Heinen et al., 2009).

The overall leaf hydraulic conductance comprises both axial water transport along xylem vessels and transcellular transport in vascular bundles and the mesophyll. In support for a transcellular path, evidence for a role of aquaporins in leaf water transport is emerging. This was first suggested by strong expression of aquaporins in bundle sheath cells (Frangne et al., 2001) or other cell types showing high water permeability (Hachez et al., 2008). In addition, the general aquaporin blocker, mercury, was able to inhibit K_{leaf} in sunflower (*Helianthus annuus*) and in six temperate deciduous trees (Aasamaa and Sober, 2005; Nardini et al., 2005). However, the concentrations used were very high ($\geq$200 μM $HgCl_2$), and the effects were not reversible. Finally, rapid and reversible changes in K_{leaf} can be induced by environmental factors such as changes in irradiance (Nardini et al., 2005; Tyree et al., 2005; Sack and Holbrook, 2006) and air and soil humidity (Nardini and Salleo, 2005; Levin et al., 2007). Pressure probe measurements in midrib parenchyma cells of corn leaves revealed that the effects of light (in addition to turgor) on leaf water transport were mediated in part through changes in cell hydraulic conductivity (Kim and Steudle, 2007). The hypothesis that rapid changes in K_{leaf} involve aquaporin regulation was further substantiated in a study in walnut trees (Cochard et al., 2007). The authors analyzed, using real-time reverse transcription (RT)-PCR, the abundance of two major PIP2 aquaporin transcripts during a transition from dark to high light and found a very good kinetic correlation between the increase in K_{leaf} and the increase in PIP2 aquaporin expression. Yet, forward or reverse genetic evidence for a role of aquaporins in leaf water transport is lacking.

Because of the limiting role of plasma membranes in transcellular water transport, plasma membrane intrinsic protein (PIP) aquaporins represent the most likely candidates for protein-mediated hydraulic conductivity in roots and leaves (Kaldenhoff et al., 2008; Maurel et al., 2008; Heinen et al., 2009). PIPs occur in two distinct clades. Antisense inhibition of PIP1 and PIP2 expression in transgenic Arabidopsis (*Arabidopsis thaliana*) and tobacco (*Nicotiana tabacum*) has indicated a general role for aquaporins of the two classes in root water transport (Kaldenhoff et al., 1998; Martre et al., 2002; Siefritz et al., 2002). More specifically, a specialized role of AtPIP2;2 in osmotic but not hydrostatic root water uptake was uncovered using T-DNA insertion mutagenesis (Javot et al., 2003). Yet, similar dissection has been lacking in the context of leaf water transport. Based on oocyte and yeast expression assays, it was inferred that PIP1 aquaporins may have, with respect to PIP2 aquaporins, a reduced water transport activity (Fetter et al., 2004; Suga and Maeshima, 2004; Sakurai et al., 2008). As a consequence, knowledge on the role of individual PIP1 isoforms in water transport in planta has been lagging.

In this work, we used Arabidopsis to investigate in detail the overall significance of PIP aquaporins to tissue water conductivity. This approach first required the development of novel water transport and pharmacological assays in excised rosettes. These and other assays allowed an accurate reverse genetic analysis of AtPIP1;2 function. This aquaporin (initially referred to as AthH2 or PIP1b) is one of the most abundant PIPs in the root and rosette (Kaldenhoff et al., 1995; Javot et al., 2003; Santoni et al., 2003; Alexandersson et al., 2005; Boursiac et al., 2005).

RESULTS

Isolation of an *AtPIP1;2* T-DNA Insertion Mutant

Expression in transgenic Arabidopsis of a chimeric gene comprising 2,248-bp sequence upstream of the *AtPIP1;2* coding region fused to a GUS coding sequence induced an intense X-Gluc staining in both roots and shoots (Fig. 1A). In roots, a staining was observed preferentially in the endodermis and stele and to a lesser extent in the cortex (Fig. 1B). A significant expression of PIP1;2:GUS was also observed in

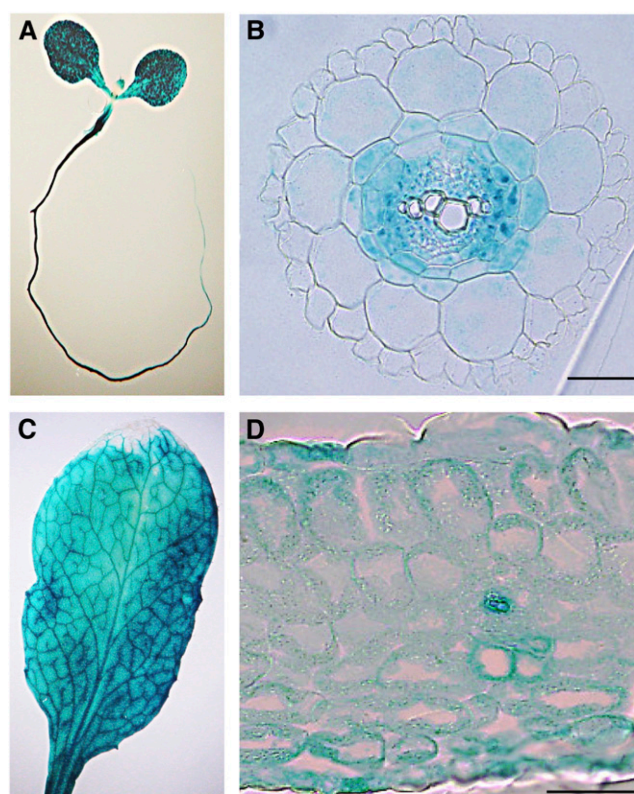

Figure 1. Expression analysis of a *PIP1;2-GUS* construct. The figure shows the GUS staining of a whole 5-d-old plant grown in vitro (A). GUS staining of a cross section at >5 mm from a root tip (B; bar =50 μm), of an entire leaf (C), or of a leaf cross section (D; bar = 50 μm) was made in a 21-d-old plant grown in hydroponic conditions.

all rosette tissues examined, including vascular bundle, bundle sheath, and lamina (epidermis, mesophyll, and stomata; Fig. 1, C and D). These observations roughly confirm a previous GUS expression study employing a somewhat shorter promoter region (Kaldenhoff et al., 1995). They agree with proteomic and transcriptomic analyses indicating that AtPIP1;2 is one of most highly expressed aquaporins in Arabidopsis (Santoni et al., 2003; Alexandersson et al., 2005; Boursiac et al., 2005).

Two transgenic Arabidopsis lines (SALK_145347 and SALK_19794), each with a T-DNA insertion within the first intron of *AtPIP1;2* (Fig. 2A), were obtained from the Nottingham Arabidopsis Stock Centre, and their genomic structure at *AtPIP1;2* was confirmed (Fig. 2B). Plants homozygous for either one of the T-DNA insertions, and hereafter referred to as *pip1;2-1* and *pip1;2-2*, were analyzed by RT-PCR. These plants lacked any chimeric *AtPIP1;2* transcript encompassing part or the entirety of the T-DNA sequence (data not shown) or any transcript with *AtPIP1;2* sequence transcribed downstream of the T-DNA insertion (Fig. 2C). Thus, expression of *AtPIP1;2* is fully knocked out in *pip1;2-1* and *pip1;2-2*. We chose *pip1;2-1* for complementation by the *At*PIP1;2 cDNA, which was placed under the control of a doubled 35S cauliflower mosaic virus promoter and was introduced into *pip1;2-1* by *Agrobacterium tumefaciens*-mediated transformation to yield *pip1;2-1Comp* lines. RT-PCR analysis showed that expression of *AtPIP1;2* transcripts was restored in these lines (Fig. 2C). Wild-type, *pip1;2-1*, *pip1;2-2*, and *pip1;2-1Comp* plants grown in vitro or in soil were morphologically undistinguishable. Root and shoot growth was also characterized in 21-d-old wild-type, *pip1;2-1*, and *pip1;2-1Comp* plants grown in hydroponic conditions. The three genotypes showed similar root dry weight (DW) and similar rosette DW and leaf surface (Table I).

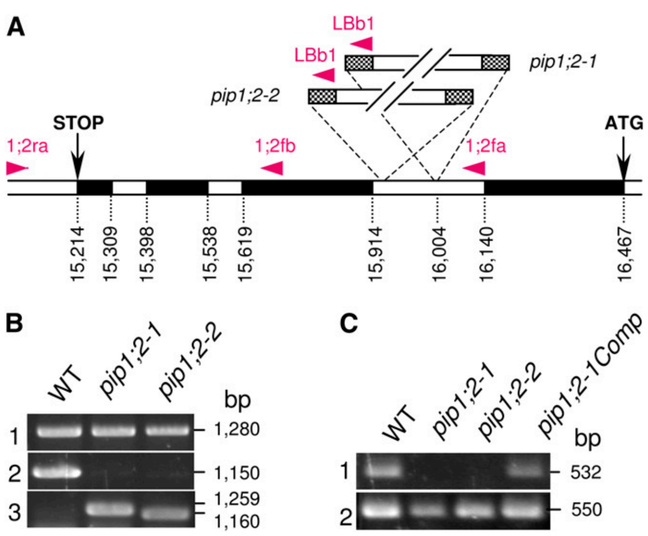

Figure 2. Molecular characterization of the *pip1;2-1* and *pip1;2-2* insertion mutants. A, Physical map of the *AtPIP1;2* gene with schematic position of the T-DNA insertions identified in the Salk_145347 and Salk_19794 lines and corresponding to *pip1;2-1* and *pip1;2-2*, respectively (see text). The initiating (ATG) and STOP codons are indicated, with exons shown in black. The numbering of nucleotides refers to the genomic sequence of *AtPIP1;2* in BAC clone F4I18. Horizontal arrowheads indicate the positions and orientations of primer sequences used for PCR analysis of the gDNA and resulting cDNA in the genotypes indicated below. B, PCR analysis of gDNA of wild-type (WT), *pip1;2-1*, and *pip1;2-2* plants using a pair of *AtPIP1;1*-specific primers (1;1f/1;1r) (1), a pair of *AtPIP1;2*-specific primers (1;2fa/1;2ra) (2), and two primers specific for *AtPIP1;2* (1;2ra) and the T-DNA (LBb1), respectively (3). C, RT-PCR analysis of *AtPIP1;2* mRNA expression in wild-type, *pip1;2-1*, *pip1;2-2*, and *pip1;2-1Comp* plants. Expression of *AtPIP1;2* cDNA was probed with primers (1;2fb/1;2ra) (1) located downstream of the T-DNA insertion site. Amplification of an Elongation Factor1α cDNA fragment was performed for controlling cDNA integrity (2). [See online article for color version of this figure.]

Contribution of AtPIP1;2 to Root Water Transport

The high expression of AtPIP1;2 in roots (Fig. 1; Kaldenhoff et al., 1995; Javot et al., 2003; Santoni et al., 2003; Alexandersson et al., 2005; Boursiac et al., 2005) prompted us to investigate its role in water uptake. The function of AtPIP2;2, another abundantly expressed root aquaporin, was previously unraveled by comparison of osmotic water transport in roots of wild-type and knockout plants (Javot et al., 2003). Using a similar assay, we collected the sap that was spontaneously exuded from roots excised from wild-type and *pip1;2-1* plants. Similar sap osmolalities (72–75 mOsmol) and sap flow rates were observed in the two genotypes, which overall indicate similar osmotic hydraulic conductivities ($Lp_{r\text{-}o}$; Table II). To investigate another mode of water transport, we used a pressure chamber device and characterized the hydrostatic pressure dependence of sap flow in roots excised from wild-type, *pip1;2-1*, and *pip1;2-1Comp* plants. Corresponding hydrostatic hydraulic conductivity values ($Lp_{r\text{-}h}$) were determined (Javot et al., 2003). With respect to wild-type and *pip1;2-1Comp* plants, *pip1;2-1* showed a statistically significant reduction in $Lp_{r\text{-}h}$ by 21% and 31%, respectively, whereas the first two genotypes did not show any statistical difference in $Lp_{r\text{-}h}$ (Fig. 3). In another set of experiments, we compared wild-type (n = 10) and *pip1;2-2* (n = 14) plants and found that the latter genotype showed a reduction in $Lp_{r\text{-}h}$ by 33% $\pm$ 4%. The overall data establish a role for AtPIP1;2 in hydrostatic water transport in the Arabidopsis root and a minor if any contribution to osmotic root water transport.

Light-Dependent Hydraulic Conductivity of the Arabidopsis Rosette (K_{ros})

To investigate the water transport properties of Arabidopsis leaf tissues, a novel procedure was developed in which whole excised rosettes that were bathing in a liquid solution were inserted into a pressure chamber. The flow rate of sap (J_v) exuded

Table I. *Morphology of wild-type, pip1;2-1, and pip1;2-1Comp plants grown in hydroponic culture*

Measured Parameter	Wild Type	*pip1;2-1*	*pip1;2-1Comp*
Root DW (mg)[a]	9.54 ± 0.77	9.77 ± 0.63	8.59 ± 0.60
	(*n* = 21)	(*n* = 19)	(*n* = 21)
Rosette DW (mg)[b]	32.07 ± 2.50	33.10 ± 2.83	37.21 ± 2.16
Rosette surface (cm^2)[b]	18.01 ± 1.37	18.57 ± 1.55	20.82 ± 1.18
	(*n* = 37)	(*n* = 31)	(*n* = 13)

[a]Data from a representative experiment in which plants of the indicated genotype were cultured in parallel. Root DW (mean value; ±SE) was measured on 21-d-old plants. Mean values in *pip1;2-1* or *pip1;2-1Comp* plants are not statistically different from value in control wild-type plants. [b]Cumulated data from four independent cultures and the indicated number of plants. Rosette DW and surface, both as mean values ± SE, were measured on 21-d-old plants. Mean values in *pip1;2-1* or *pip1;2-1Comp* plants are not statistically different from value in control wild-type plants.

from the sectioned hypocotyl of an individual plant was proportional to the applied pressure (P) and intercepted the P axis at a balancing pressure close to the origin (P_0 = 0.016 ± 0.003 MPa; n = 39; Fig. 4A). Sap exudation was substantially increased (>2-fold) upon successive section of all leaf blades (Supplemental Fig. S1), suggesting that leaf petioles and blades equally contribute to the hydraulic resistance of the whole rosette. In addition, the $J_v(P)$ relationship was shifted toward higher pressures, with an increase in P_0 by approximately 0.1 MPa, when a PEG6000 concentration equivalent to 0.1 MPa was added to the rosette bathing solution. These results suggest that under our experimental conditions, the whole rosette could be assimilated to an osmotic barrier. From the slope of the $J_v(P)$ relationship, a rosette hydraulic conductivity value (K_{ros} ± SE) of 149.5 ± 8.7 μL s^{-1} m^{-2} MPa^{-1} (n = 47) was deduced.

Initial measurements were performed during the day (16-h period at 250 μmol photons m^{-2} s^{-1}) in rosettes excised >3 h after the onset of light. Because leaf hydraulic conductance is dependent on irradiance in most of plant species investigated (Tyree et al., 2005; Sack and Holbrook, 2006), we also investigated K_{ros} in rosettes excised during the night. A tendency (probability = 0.07) to an increase in K_{ros} by 38.2% ± 18.2% was observed (Fig. 4B). To possibly observe more marked effects, plants were maintained under darkness by prolonging a normal night by periods of 3 to 10 h. In these conditions, $J_v(P)$ relationships comparable to those recorded in rosettes excised during the day could be recorded (Fig. 4A). Yet, a significant increase (probability = 0.009) in slope was observed, yielding an 88.6% ± 22.4% increase in K_{ros} (Fig. 4B). The dependence of K_{ros} on plant growth conditions supports the idea that this parameter reflects true physiological properties of the Arabidopsis rosette.

Similar to other high-pressure methods, our measurements rely on the principle that under conditions of pressure-induced flow of liquid water the hydraulic resistance of stomatal pores is not limiting with respect to that of internal leaf structures with much smaller conducing diameters (Tyree et al., 2005). Porometer measurements showed that water stomatal conductance (g_s ± SE; n = 18 plants) of plants at midday or after exposure to extended darkness were 539 ± 33 mmol s^{-1} m^{-2} and 90 ± 19 mmol s^{-1} m^{-2}, respectively. Thus, an increase in K_{ros} was observed in conditions with the lowest g_s. These results confirm that, even in conditions of reduced aperture, stomatal pores are not limiting barriers for pressure-dependent liquid flow across the whole rosette.

Effects of Aquaporin Inhibitors on K_{ros}

To test for the contribution of aquaporins to K_{ros}, we first investigated the effects of the common aquaporin blocker, mercury, in conditions where K_{ros} was maximal. Figure 5A shows that in rosettes excised from plants subjected to an extended darkness treatment, exposure to a bathing solution containing 50 μM $HgCl_2$ induced a time-dependent decrease in $J_v(P)$ (Fig. 5A), leading to mean inhibition of K_{ros} by 26.3 ± 4.1% (n = 18; Fig. 6A), with a half-time of $t_{1/2}$ = 17.8 ± 2.6 min. Azide (NaN_3) was previously shown to induce cell acidosis and, therefore, a pH-dependent closure of PIP aquaporins in Arabidopsis roots (Tournaire-Roux et al., 2003). Treatment of the rosette with 2 mM NaN_3 induced a decrease in $J_v(P)$, which was very similar in amplitude (23.1% ± 3.7%; n = 17) and time dependency ($t_{1/2}$ = 27.3 ± 4.3 min) to the mercury-induced effects (Figs. 5B and 6A). Noticeably, this inhibition could be reversed at 82.8% ± 9.6% and with a $t_{1/2}$ = 21.5 ± 3.4 min upon washout of the inhibitor,

Table II. *Osmotic water transport in roots excised from wild-type and pip1;2-1 plants*

Measured Parameter	Wild Type (n = 20)[a]	*pip1;2-1* (n = 28)[a]
Sap osmolality (mOsmol)[b]	75.0 ± 4.2	72.2 ± 2.3
$Lp_{r\text{-}o}$ (mL g^{-1} h^{-1} MPa^{-1})[c]	41.7 ± 5.1	41.4 ± 4.1

[a]Cumulated data from three independent cultures and the indicated number of plants. [b]Mean osmolality (±SE) of sap exuded from excised roots. Values of wild-type and *pip1;2-1* plants are not statistically different. [c]Mean root osmotic hydraulic conductivity (±SE). Values of wild-type and *pip1;2-1* plants are not statistically different.

indicating that the NaN_3 treatment had no irreversible effect on leaf structure or metabolism. By contrast, mercury-induced inhibition of K_{ros} could not be reversed after washout of the inhibitor (1.7% ± 3.0% at 60 min; $n = 6$).

In rosettes collected during the day, both 50 μM $HgCl_2$ and 2 mM NaN_3 induced an inhibition of $J_v(P)$ with time dependencies similar to those observed in rosettes from dark-grown plants (data not shown). The extent of K_{ros} inhibition was similar with the two treatments ($HgCl_2$, 12.9% ± 1.9%; NaN_3, 14.5% ± 1.8%; Fig. 6B) but was significantly lower than in rosettes from plants exposed to extended darkness.

The overall data show that two aquaporin inhibitors, with distinct modes of action, were able to induce similar inhibition of K_{ros}. We also note that the relative effects were the highest in conditions where K_{ros} was the highest (extended darkness, K_{ros} = 261 ± 45.4 μL s^{-1} m^{-2} MPa^{-1}; light, K_{ros} = 128.7 ± 8.7 μL s^{-1} m^{-2} MPa^{-1}). Thus, the absolute blocking effects of both azide and mercury on K_{ros} were nearly 4 times as high in rosettes from plants subjected to extended darkness than in rosettes from light-grown plants (Fig. 6).

Effects of the Light Regime on *PIP* Gene Expression

To investigate further the effects of the light regime of leaf aquaporin function, we monitored the expression of all 13 *AtPIP* genes in leaves of plants grown under light or extended darkness. For this, we used gene-specific primer pairs and quantified the abundance of *AtPIP* transcripts using real-time RT-PCR analysis in three independent biological experiments (plant cultures). Figure 7 shows the expression ratio of each *AtPIP* between extended darkness and light. Four genes, including *AtPIP1;2* and *AtPIP2;6*, showed an approxi-

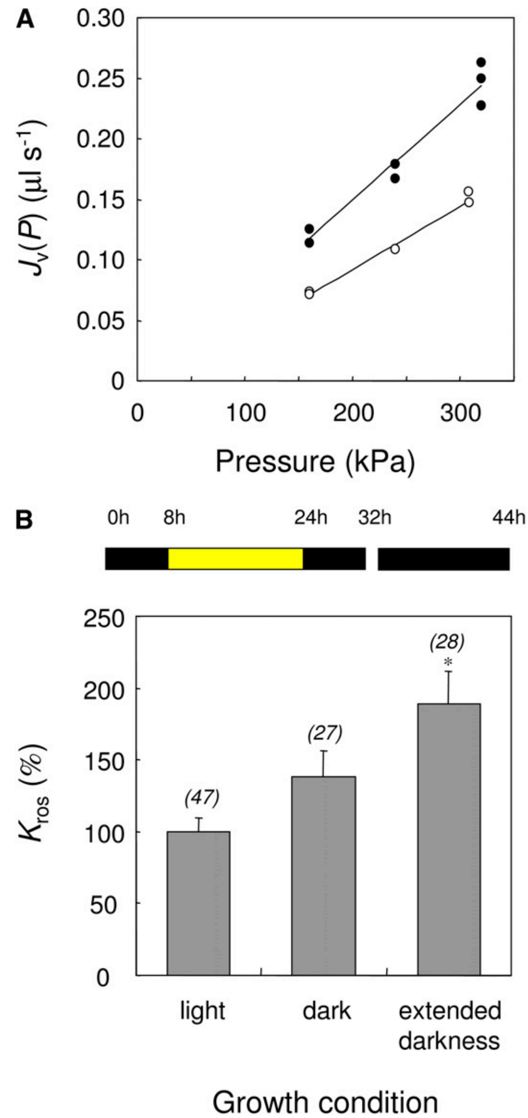

Figure 4. Effects of the irradiance regime on rosette hydraulic conductivity (K_{ros}). A, Representative pressure-to-flow relationships measured in rosettes from plants grown under a normal photoperiodic regime and collected around midday (photosynthetically active radiation = 250 μmol photons m^{-2} s^{-1}; white circles) or plants exposed to a prolonged night (11–21 h darkness; extended darkness; black circles). In both cases, excised rosettes were submerged into a bathing solution, inserted into a pressure chamber, and the flow of sap exuding from the sectioned hypocotyl [$J_v(P)$] was measured at the indicated pressure as described in "Materials and Methods." The slope of the regression line is indicative of rosette hydraulic conductance, and together with the cumulated leaf surface allows calculating rosette hydraulic conductivity values (white circles, K_{ros} = 141.2 μL s^{-1} m^{-2} MPa^{-1}; black circles, K_{ros} = 223.4 μL s^{-1} m^{-2} MPa^{-1}). B, K_{ros} from plants grown under a normal photoperiodic regime (16 h light/8 h dark) and measured around midday (light) or during the night (dark). K_{ros} was also measured in plants exposed to an extended darkness (see text and schematic representation above). K_{ros} was expressed as percentage of the mean control value measured in the light (K_{ros} = 149.5 μL s^{-1} m^{-2} MPa^{-1}). The number of individual plants measured in each condition is indicated, and the asterisk indicates a statistically significant difference from control values (probability = 0.009). [See online article for color version of this figure.]

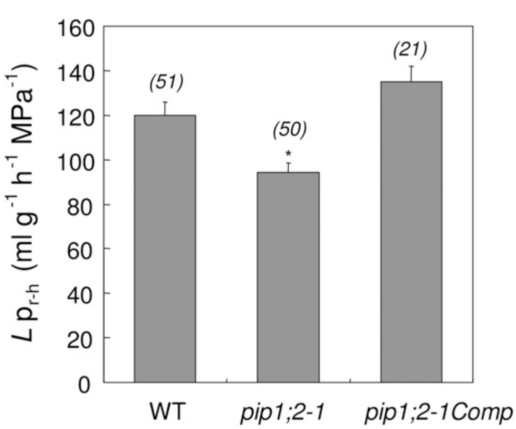

Figure 3. Mean hydrostatic hydraulic conductivity of roots ($Lp_{r\text{-}h}$) from wild-type (WT), *pip1;2-1*, and *pip1;2-1Comp* plants. $Lp_{r\text{-}h}$ was measured during the daytime in plants grown under a normal photoperiodic regime. Data were pooled from four independent cultures and the indicated number of plants. Values are means ± SE, and the asterisk indicates a statistically significant difference (probability < 0.002) from the wild-type value.

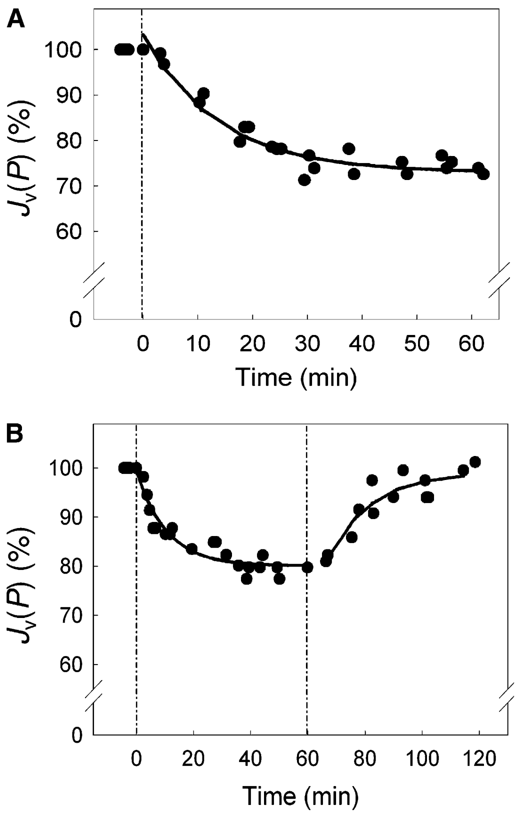

Figure 5. Time-dependent effects of aquaporin blocking treatments on pressure-induced water transport in rosettes from plants grown under extended darkness. A, Effects of exposure to mercury. An excised rosette was subjected to a constant pressure (P = 0.32 MPa), and $J_v(P)$ was measured over time. The bathing solution was complemented with 50 μM $HgCl_2$ at time t = 0. Fit of the kinetic data by a first-order exponential function indicated a final inhibition of 26.7% with a half-time ($t_{1/2}$) of 11.4 min. B, Effects of exposure to azide. Same procedure as in A except that 2 mM NaN_3, instead of mercury, was added to the bathing solution at t = 0 and was removed after 60 min. The fitted data indicate a maximal inhibition of 19.9%, with a $t_{1/2}$ = 6.2 min. Reversion occurred with a fitted amplitude of 98.9% and $t_{1/2}$ of 14.4 min.

mately 2-fold increase in transcript abundance under darkness. *AtPIP2;1*, which is also highly expressed in leaves (Alexandersson et al., 2005), *AtPIP1;4*, and *AtPIP2;8* were, by contrast, repressed under prolonged darkness. All remaining genes showed a fairly stable expression between the two conditions. The data suggest a complex interplay of PIP isoform function and regulation to determine the hydraulic properties of leaves under various light regimes.

Contribution of AtPIP1;2 to K_{ros}

The contribution of AtPIP1;2 to K_{ros} was investigated in plants grown under extended darkness because they exhibit the possibly highest activity of leaf aquaporins (Fig. 6) and of AtPIP1;2 in particular (Fig. 7). Pooled data from four independent series of measurements indicated for wild-type and *pip1;2-1* plants mean K_{ros} values (μL s^{-1} m^{-2} MPa^{-1} $\pm$ SE) of 216.7 $\pm$ 13.4 (n = 44 plants) and 171.4 $\pm$ 6.9 (n = 38 plants), respectively. These results indicate a statistically significant (probability = 0.003) reduction of K_{ros} by 21% in *pip1;2-1* with respect to the wild type. Figure 8 shows a representative experiment in which the K_{ros} of *pip1;2-1Comp* plants was characterized in parallel to that of the two former genotypes. K_{ros} of *pip1;2-1Comp* was significantly higher than that of *pip1;2-1* but similar to the K_{ros} of wild-type plants. The overall data provide evidence that AtPIP1;2 transports water in inner leaf tissues of plants. Because the extent of K_{ros} inhibition in AtPIP1;2 knockout with respect to wild-type plants is in the same range as the extent of K_{ros} inhibition by mercury and azide, the data further suggest that AtPIP1;2 can account for a significant portion of aquaporin-mediated leaf water transport in plants grown under extended darkness.

Contribution of AtPIP1;2 to the Water Permeability of Mesophyll Protoplasts

The K_{ros} is determined by the axial conductance of xylem vessels in the petiole and leaf blades and by the

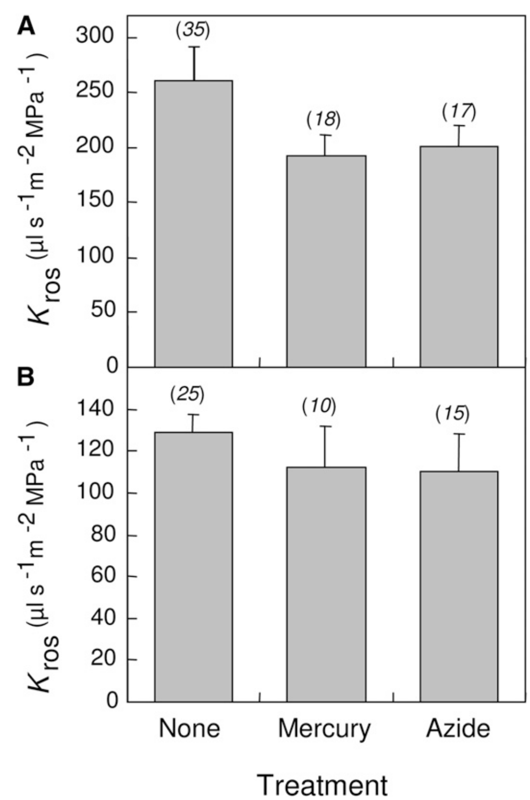

Figure 6. Effects of aquaporin blockers on K_{ros} of plants grown under extended darkness (A) or in the light under a normal photoperiodic regime (B). K_{ros} was measured in excised rosettes before (none) and after treatment for 60 min with mercury (50 μM $HgCl_2$) or azide (2 mM NaN_3). Data were cumulated from at least four independent cultures, with the indicated number of plants.

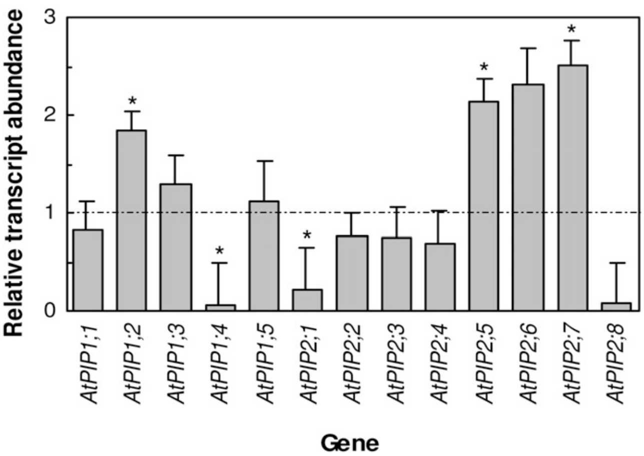

Figure 7. Effects of the light regime on the expression of *AtPIP* genes in the Arabidopsis rosette. The transcript abundance of each *AtPIP* gene in whole rosettes was measured by real-time RT-PCR as explained in "Materials and Methods." The figure shows the mean expression ratio between plants grown under extended darkness and plants grown in the light under a normal photoperiodic regime. Cumulated data (±SE) are from three independent biological experiments, each with duplicate PCR reactions. Asterisks indicate significant effects (probability < 0.05) of the light regime.

conductance of apoplastic and cell-to-cell paths in the vascular bundles and the mesophyll. To estimate the contribution of AtPIP1;2 to cell water transport in the latter tissue, we used a previously described swelling assay in isolated mesophyll protoplasts (Ramahaleo et al., 1999; Martre et al., 2002). More specifically, the protoplast water permeability (P_f) was compared in wild-type, *pip1;2-1*, and *pip1;2-2* plants grown under prolonged darkness. In these conditions, wild-type protoplasts showed broadly distributed P_f values, with a majority of protoplasts with low values ($P_f <$ 8 μm s^{-1}) and a significant subclass with higher values (Fig. 9A). In protoplasts from the two knockout lines, P_f values were less scattered, the subpopulation of protoplasts with high P_f being markedly reduced (Fig. 9A). As a result, mean P_f in these lines was 2-fold lower than in the wild type (Fig. 9B). The data suggest that AtPIP1;2 contributes to water transport in mesophyll cells, this function being the most apparent in the protoplasts with the highest P_f (aquaporin activity).

DISCUSSION

PIP1;2 Contributes to Root Water Transport

Previous studies (Kaldenhoff et al., 1995, 1998; Martre et al., 2002; Siefritz et al., 2002) have addressed the water transporting role of PIP1 homologs using antisense gene expression in transgenic plants. A decrease in leaf protoplast water permeability and, most remarkably, an enhanced growth of roots was observed in transgenic Arabidopsis materials (Kaldenhoff et al., 1998; Martre et al., 2002). The latter phenotype was tentatively interpreted as a compensation for reduced root water permeability to maintain plant water uptake capacity. In support of this, Siefritz et al. (2002) observed a reduced Lp_r in tobacco plants expressing the antisense copy of a PIP1 (NtAQP1) cDNA. Aharon et al. (2003) have used another strategy and investigated the function of AtPIP1;2, one of most abundantly expressed PIP1 isoforms in Arabidopsis, by overexpression in tobacco. Transgenic plants showed a spectacular enhancement of growth under favorable conditions but accelerated wilting under drought conditions. It remains unclear, however, whether this phenotype was due to true hydraulic effects of AtPIP1;2 in tobacco tissues, to an indirect stomatal deregulation, or to other unknown effects induced by heterologous expression.

In this work, we used a knockout approach to address the function of AtPIP1;2. Macroarray analysis of aquaporin gene expression (Boursiac et al., 2005) showed that the lack of AtPIP1;2 was not compensated for by changes in expression of any other isoforms (data not shown). Because interactions between PIP isoforms can interfere with their subcellular trafficking (Zelazny et al., 2007), the possibility remains that functional expression of other isoforms at the plasma membrane was altered in *PIP1;2* knockout plants. Nevertheless, no alteration in plant growth was observed in the *pip1;2-1* mutant both under normal (Table I) and salt stress conditions (data not shown). Yet, disruption of AtPIP1;2 had significant effects (20%–30%) on the root hydrostatic hydraulic conductivity ($Lp_{r\text{-}h}$). By contrast, osmotic water transport ($Lp_{r\text{-}o}$), as assayed by spontaneous exudation of excised roots, was not altered in *pip1;2-1*. This phenotype

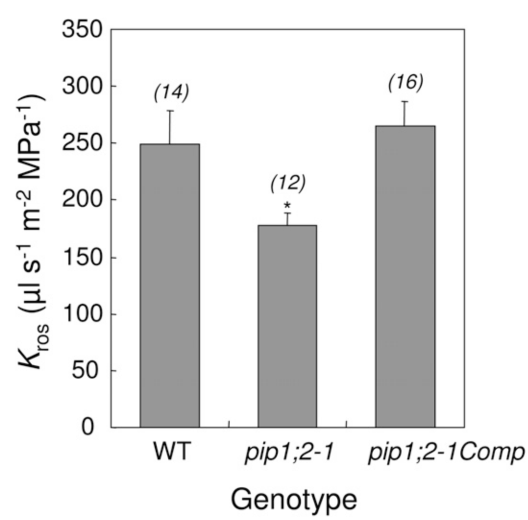

Figure 8. K_{ros} of wild-type (WT), *pip1;2-1*, and *pip1;2-1Comp* plants grown under extended darkness conditions. K_{ros} was measured on the indicated number of plants, as exemplified in Figure 4. Values are means ± SE, and the asterisk indicates a statistically significant difference from the wild-type value.

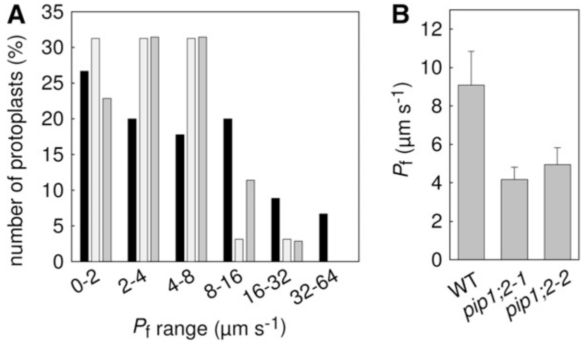

Figure 9. P_f of mesophyll protoplasts isolated from wild-type (WT), *pip1;2-1*, and *pip1;2-2* plants grown under extended darkness conditions. Cumulated data are from four protoplast preparations from two independent plant cultures (wild type, $n = 45$; *pip1;2-1*, $n = 32$; *pip1;2-2*, $n = 35$). A, Relative distribution of P_f values in wild-type (black bars), *pip1;2-1* (empty bars), and *pip1;2-2* (gray bars) protoplasts. B, Mean P_f values ($\pm$SE).

differs from that of previously described AtPIP2;2 knockout mutants, which showed a significant alteration in osmotic but not in hydrostatic pressure-dependent water transport (Javot et al., 2003).

Because osmotic gradients within the root determine its exudation capacity, $Lp_{r\text{-}o}$ exclusively involves membrane water transport pathways. Pharmacological evidence showed that 80% to 90% of Arabidopsis $Lp_{r\text{-}h}$ can also be accounted for by aquaporin activities (Tournaire-Roux et al., 2003), meaning that, even under a purely hydrostatic driving force, the apoplastic path has a modest contribution in this species. Thus, both $Lp_{r\text{-}o}$ and $Lp_{r\text{-}h}$ result from the integrated water transport capacity of concentric cell layers acting in series. The two parameters were derived, however, from assays differing by the nature and intensity of the local driving forces driving radial water transport. Depending on the assay, the limitation of a cell layer may therefore be purely hydraulic ($Lp_{r\text{-}h}$) or may also depend on its ability to generate a local osmotic driving force ($Lp_{r\text{-}o}$) through solute pumping activity and cell wall tightness. Within this representation, our experimental results suggest a model whereby various root aquaporin isoforms are specialized in distinct modes of water transport, through preferential expression and/or regulation in cell layers with a specialized anatomy and membrane transport protein equipment. It is striking that, although the expression patterns of *AtPIP1;2* and *AtPIP2;2* in roots are somewhat overlapping, the corresponding knockout phenotypes were so distinct (Javot et al., 2003; this work). This result will certainly stimulate complementary studies, which should combine a thorough analysis of aquaporin expression patterns to cell and whole-root transport assays in a larger number of aquaporin mutant plants and should lead to an integrative modeling of root water transport.

Pressure Chamber Measurements of the Rosette Hydraulic Conductivity (K_{ros})

Due to the small size of individual Arabidopsis leaves, high-pressure methods commonly used to measure K_{leaf} cannot be easily applied to this species. In this work, we used whole excised rosettes bathing in a liquid solution and inserted into a pressure chamber. The whole rosette forms a hydraulic network that is definitely more complex than that of a single leaf. Both systems integrate vascular and nonvascular resistances. Here, we show that leaf petioles and blades each contributed to about one-half of the rosette hydraulic resistance (Supplemental Fig. S1). Sack et al. (2002) established the equivalence of K_{leaf} measurement methods in which trans-leaf water flow was induced by high-pressure, evaporation, or vacuum. The K_{ros} values reported in this work compare properly with the range of K_{leaf} values measured in Arabidopsis by an evaporative method (Martre et al., 2002) or in other plant species (Sack and Holbrook, 2006). However, other K_{leaf} values determined in Arabidopsis, also by an evaporative method (Levin et al., 2007), were noticeably lower. One difference was that plants were grown at much lower light (120 μmol photons m^{-2} s^{-1}) than in the work by Martre et al. (2002) (200 μmol photons m^{-2} s^{-1}) or in this study (250 μmol photons m^{-2} s^{-1}). Nevertheless, calculations based on Poiseuille's law have shown that, by comparison to inner leaf tissues, stomata do not exert a significant hydraulic limitation in high-pressure measurements as used in this work (Tyree et al., 2005). In agreement with these theoretical considerations, we were able to detect a 2-fold increase in K_{ros} in conditions where stomatal aperture was reduced by approximately 83%. The significance of our measurements with respect to physiological leaf water transport and aquaporin function was also assessed, as discussed below, by several lines of evidence, including reduction of K_{ros} by aquaporin inhibitors and in aquaporin knockouts or regulation of K_{ros} by light.

Pharmacological and Genetic Evidence for a Role of Aquaporins in Leaf Water Transport

An inhibition of K_{leaf} by mercury has been reported in sunflower and several tree species and coincided with the highest light-dependent or seasonal K_{leaf} values (Aasamaa and Sober, 2005; Nardini et al., 2005). However, the significance of this inhibition has remained uncertain because of the high mercury concentrations needed and its lack of reversibility. This work shows consistent effects of two aquaporin inhibitors, at lower concentration and with independent modes of action in two contrasting physiological contexts, that is, under light and extended darkness. The finding that the inhibiting effects of azide were reversible further substantiated our pharmacological approach.

Although reverse genetics can be more straightforward to definitely establish a role of aquaporins in leaf

Table III. *Sequence of PIP-specific primer pairs used for real-time RT-PCR amplification*

All primers were designed in the 3′ untranslated transcribed region. The numbers refer to positions from the initiating ATG codon in the genomic sequences. Primers with an asterisk were similar to those designed by Jang et al. (2004).

Gene	Primer	Amplicon Size
		bp
AtPIP1;1	Forward*: 5′-^{1487}CTGGCCTTGTCCTTAGTTGCTTC^{1510}-3′ Reverse: 5′-^{1613}TCTCCTTTGGAACTTCTTCCTTG^{1590}-3′	126
AtPIP1;2	Forward: 5′-^{1346}TCCTCTTCTTTGCCTAATGGAGAC^{1370}-3′ Reverse: 5′-^{1478}AGTTGCCTGCTTGAGATAAAC^{1457}-3′	132
AtPIP1;3	Forward: 5′-^{1312}GCTGTGGATGATCTGGTTTTATCG^{1336}-3′ Reverse: 5′-^{1486}GCCGAAACAATATGGATCTTACTC^{1462}-3′	174
AtPIP1;4	Forward: 5′-^{1591}CTCTGAAGTCTAAGGTGATTAGTGC^{1616}-3′ Reverse: 5′-^{1708}CAACCCGAGAACTTGATGTTGA^{1686}-3′	117
AtPIP1;5	Forward: 5′-^{1436}TGTTTCCTATGTCATGTGTGATG^{1459}-3′ Reverse: 5′-^{1582}GTACACAATGTATTCTTCCATTGAC^{1557}-3′	146
AtPIP2;1	Forward: 5′-^{1647}TGTGTTTTCCACTTGCTCTTTTG^{1670}-3′ Reverse: 5′-^{1765}CACAACGCATAAGAACCTCTTTGA^{1741}-3′	120
AtPIP2;2	Forward: 5′-^{1247}GGCAACTTTGCTTGTAAAACTATGC^{1295}-3′ Reverse: 5′-^{1349}AGTACACAAACATTGGCATTGG^{1327}-3′	102
AtPIP2;3	Forward: 5′-^{1199}GAAACATATCCTCTTTTCCACTCG^{1224}-3′ Reverse: 5′-^{1333}CTCAATACACCAAACTTACATACG^{1309}-3′	134
AtPIP2;4	Forward: 5′-^{1245}CTCCTTTAGGAGCTTTGCTTAAT^{1268}-3′ Reverse*: 5′-^{1437}CCACATTTACAATTACACGAATGG^{1414}-3′	192
AtPIP2;5	Forward*: 5′-^{1626}GATATGCTCTTCCCTGAGTACATC^{1650}-3′ Reverse*: 5′-^{1769}AATATCTCTCCTCACCAAAGCTAG^{1745}-3′	143
AtPIP2;6	Forward*: 5′-^{2191}TTTCGAACTAGCGAAGAGGTGAAG^{2215}-3′ Reverse: 5′-^{2324}AGACACAGTAAATGTCACTCACC^{2301}-3′	133
AtPIP2;7	Forward: 5′-^{1364}TGTGTAATGAGAGAGATGGTGGA^{1387}-3′ Reverse: 5′-^{1476}AGAGAAACCAAAGGCAAACGA^{1455}-3′	112
AtPIP2;8	Forward: 5′-^{1518}CAACCCAACCAATTGATGATTCA^{1541}-3′ Reverse: 5′-^{1687}ACATGAAAGAAAGCAACGGAC^{1666}-3′	169

water transport (Martre et al., 2002; Siefritz et al., 2002; Aharon et al., 2003), conclusive studies have been lacking so far. The prerequisite to a knockout approach was to identify the isoforms that are the most highly expressed in leaves. Expression profiling of the aquaporin family has shown that *AtPIP1;2*, *AtPIP2;1*, and *AtPIP2;6* are among the most highly expressed *PIP* genes in the Arabidopsis rosette (Alexandersson et al., 2005). Consistent with this, we found that, under extended darkness conditions, AtPIP1;2 can contribute to up to 21% of K_{ros}. As discussed above in the context of the root, the water transport phenotype of *AtPIP1;2* knockout rosettes establishes that a genetic dissection of water transport paths and cell hydraulics in leaves has become feasible. We also found that, in accordance to other leaf systems, the Arabidopsis K_{ros} likely integrates a significant axial resistance of vessels, which do not involve aquaporin functions (Sack and Holbrook, 2006). Bundle sheath and mesophyll cells likely represent the other two limiting barriers to liquid water flow (Heinen et al., 2009). We note that AtPIP1;2 was expressed in these two cell types. Whereas water permeability of bundle sheath cells is hardly accessible in Arabidopsis, we tentatively estimated the contribution of AtPIP1;2 to water transport in the mesophyll by measuring the P_f of isolated mesophyll protoplasts. We realize that, in our experimental conditions, most of these cells show a low P_f, suggesting that aquaporins were possibly lowly active in this tissue or down-regulated during protoplast preparation. Nevertheless, the reduced P_f in *AtPIP1;2* knockout protoplasts points to a role of AtPIP1;2 in mesophyll water transport. Similar studies, combining expression analysis and phenotypic characterization of knockout mutants for other aquaporin isoforms, will allow us to delineate their respective contributions to water transport in various leaf tissues.

Light-Induced Changes in K_{leaf}

In this work, we also show that exposure of Arabidopsis plants to darkness increased K_{ros} and its mercury- and azide-sensitive components. Consistent with these effects, a dark treatment enhanced the transcript abundance of several aquaporin genes, including *AtPIP1;2*. Transcription of certain aquaporin genes has been reported to be under diurnal control (Smith et al., 2004; Bläsing et al., 2005). Because a prolonged darkness induced a further increase in K_{ros}, our data suggest that K_{ros} was not strictly governed by an endogenous circadian mechanism. We also note that the enhancement of *PIP* transcript abundance was moderate (≤2-fold) and that other aquaporin transcripts were down-regulated. Therefore, other mechanisms than transcriptional control may be at work to enhance K_{ros} during darkness.

Diurnal changes in K_{leaf} have been reported in numerous species, but, in most cases, K_{leaf} was increased during the day, concomitantly to a higher transpiration demand (Nardini et al., 2005; Tyree et al., 2005; Sack and Holbrook, 2006; Cochard et al., 2007). A midday depression of K_{leaf} has been reported in a tropical tree species (*Simarouba glauca*; Brodribb and Holbrook, 2004), but in this case, it was due to a vulnerability of the vascular system to cavitation rather than aquaporin regulation. Therefore, the aquaporin-mediated increase of Arabidopsis K_{ros} at night is somehow atypical. It has been proposed that a high K_{leaf}, contributed by both xylem vessel conductance and aquaporins, can improve the hydraulic linkage between leaf compartments (for instance, veins and epidermal cells; Ye et al., 2008). As leaf growth can be hydraulically limited (Ehlert et al., 2009; Parent et al., 2009), an aquaporin-mediated increase in Arabidopsis K_{ros} during the night may favor the equilibration of leaf water potentials to prepare the leaf to a metabolically controlled peak of growth right after dawn (Wiese et al., 2007).

Whereas most studies have pointed to dominating effects of light (Sack and Holbrook, 2006; Heinen et al., 2009), the physiological regulations of K_{leaf} in many species seem to be actually governed by multiple environmental factors. For instance, cell hydraulic conductivity (Lp_{cell}) in midribs of figleaf gourd (*Cucurbita ficifolia*) cotyledons and maize (*Zea mays*) leaves (Kim and Steudle, 2007; Lee et al., 2008) was enhanced by both light and high turgor. Overall, leaf water transport was enhanced under low irradiance, i.e. at reduced transpiration, due to a dominating effect of turgor over that of light. By contrast, the two effectors had antagonizing effects under transpiring conditions during the day. In Arabidopsis, the situation seems to be somewhat paradoxical. Studies with plants varying in growth conditions, or exhibiting different abscisic acid concentration or responsiveness, showed that mesophyll protoplast water permeability was strongly correlated to the plant transpiration regime and was maximal at reduced transpiration (Morillon and Chrispeels, 2001). Levin et al. (2007) found by contrast that K_{leaf} was increased at low relative air humidity that is in conditions where transpiration was the highest. At variance with these results, we observed that K_{ros} was independent from the relative air humidity in which the plants were grown and, in particular, was unchanged at saturating vapor (data not shown). Thus, K_{ros} was truly controlled by irradiance. It is important to note that these different studies where performed on somewhat distinct systems, that is, mesophyll protoplasts (Morillon and Chrispeels, 2001), single leaves (Levin et al., 2007), or excised rosettes (this work).

CONCLUSION

The low or even missing apparent water transport activity of several PIP1 aquaporins after functional heterologous expression has led to the common assumption that PIP1s are poor water channels. Here, we show that AtPIP1;2 significantly contributes to the hydraulic conductivity of both roots and rosette and therefore represents a key component of whole-plant hydraulics. Interestingly, a role in leaf CO_2 transport has been proposed for the tobacco homolog NtAQP1 (Flexas et al., 2006; Uehlein et al., 2008). The transport selectivity of AtPIP1;2 and the mechanisms that determine its transport activity and its transcriptional control by multiple factors, including blue light and abscisic acid (Kaldenhoff et al., 1993), will therefore deserve further attention. Importantly, this work, in complement to a previous study (Javot et al., 2003), underscores the power of aquaporin reverse genetics using defined mutants for dissecting the cellular components of plant hydraulics.

MATERIALS AND METHODS

Plant Cultures

All experiments were performed using Arabidopsis (*Arabidopsis thaliana*) ecotype Columbia. Seeds were surface-sterilized, kept for 2 d at 4°C, and grown in clear polystyrene culture plates at 22°C in the light for 11 d, as described (Javot et al., 2003). Seedlings were then transferred to hydroponic culture. Plants were mounted on a 35 × 35 × 1.8-cm polystyrene raft floating on a basin filled with 8 L of culture medium [1.25 mM KNO_3, 0.75 mM $MgSO_4$, 1.5 mM $Ca(NO_3)_2$, 0.5 mM KH_2PO_4, 50 μM FeEDTA, 50 μM H_3BO_3, 12 μM $MnSO_4$, 0.70 μM $CuSO_4$, 1 μM $ZnSO_4$, 0.24 μM MoO_4Na_2, and 100 μM Na_2SiO_3]. Cultures were maintained at a relative humidity of 70% with a 16-h-light (250 μmol photons m^{-2} s^{-1}) at 22°C/8-h-dark at 21°C cycle, and the culture medium was replaced each week.

For root pressure chamber and root exudation experiments, plants were used 11 to 15 d and 18 to 23 d after transfer in hydroponic conditions, respectively. For leaf water transport assays, plants were used 11 to 15 d after transfer in hydroponic conditions. Plants collected at least 3 h after the onset of the light or night periods were referred to as plants grown in the light or in the dark, respectively. To further investigate the effects of darkness, plants were transferred on the day before measurement, at the end of the photoperiod, into another growth chamber with similar relative humidity and temperature cycle as above, but under complete darkness. Plants were maintained in this chamber for 11 to 21 h before being assayed for leaf water transport. This growth condition was referred to as extended darkness. For real-time RT-PCR experiments, plants were used 12 to 13 d after transfer to hydroponic conditions. Leaves from three to four plants were excised after either a 6-h-light or 14-h-dark period, frozen in liquid nitrogen, and stored at −80°C until RNA extraction.

Molecular Characterization and Complementation of a PIP1;2 T-DNA Insertion Mutant

The Arabidopsis lines SALK_145347 and SALK_19794 were obtained from the Nottingham Arabidopsis Stock Centre (Alonso et al., 2003). The T-DNA insertions in *AtPIP1;2* were confirmed by PCR on plant genomic DNA (gDNA) using a combination of primers specific for the T-DNA left border (LBb1: 5′-GCGTGGACCGCTTGCTGCAACT-3′) and *AtPIP1;2* (1;2ra: 5′-AGTTGCCTGCTTGAGATAAACC-3′). The NPTII selectable marker was probably silenced in SALK 145347 as no kanamycin resistance was observed in this line. The line was backcrossed three times with the wild-type parental line and self-pollinated. Two homozygous lines, named *pip1;2-1* and *pip1;2-2*, were identified from SALK_14347 and SALK_19794, respectively, by PCR on gDNA using 1;2ra in combination with a 1;2fa primer (5′-AGTTCACTGGTTTCTCCGAT-3′). Integrity of *AtPIP1;1* was checked using two gene-specific primers (1;1f, 5′-ACTTCTCCAAGTATACGCCTT-3′; 1;1r, 5′-CGAAATAATTCTCCTTTGGAAC-3′). The absence of functional RNA in *pip1;2-1* and *pip1;2-2* was checked by RT-PCR using a combination of two *AtPIP1;2*-specific primers (1;2ra and 1;2fb, 5′-AACCTTTGTCCTTGTTTA-

CACC-3′). The cDNA matrix was obtained from RNAs isolated using a Svtotal RNA isolation system (Promega) after reverse transcription with a M-MLV reverse transcriptase (Promega) according to the manufacturer's instructions. Expression of the Elongation Factor1α gene was controlled as described (Javot et al., 2003).

The cauliflower mosaic virus 35S[2] expression cassette of a pKYLX 71 vector (Schardl et al., 1987) was excised with *Eco*RI and *Cla*I and introduced into a pBSKII$^+$ vector (Stratagene), with its *Sac*I, *Xba*I, and *Xho*I sites inactivated. The full-length AtPIP1;2 cDNA was PCR amplified from a pCDM8::PIP1;2 plasmid (Kammerloher et al., 1994) and subcloned into the *Xho*I site of the modified pBSK vector. The resulting construct was excised using *Eco*RI and *Cla*I and subcloned in the corresponding sites of a pGreenII 00179 vector (Hellens et al., 2000). The resulting plasmid was introduced into an *Agrobacterium tumefaciens* GV3101 strain and used to transform *pip1;2-1* by the floral dip method (Clough and Bent, 1998). Hygromycin-resistant plants were self-crossed, and T3 mono-insertional homozygous plants were selected. Transformed plants were screened for expression of AtPIP1;2 by ELISA test using an anti-PIP1 antibody (Santoni et al., 2003) on total protein extracts from 10-d-old in vitro seedlings.

GUS Reporter Construct and Histochemical Analyses

A *PIP1;2* promoter fragment encompassing 2,248 bp upstream of the start codon was cloned via GATEWAY recombination into pBGWFS7 (Karimi et al., 2002). The construct results in a translational fusion of five N-terminal amino acids of PIP1;2 with the vector-encoded GFP-GUS fusion protein. Arabidopsis Columbia-0 plants were transformed using floral dip (Clough and Bent, 1998), and independent transgenic lines were selected on soil by herbicide (BASTA) spraying. T2 generation plants were used for histochemical analyses. Staining for GUS enzyme activity was performed in two independent transformed lines on 5-d-old in vitro plantlets or on roots and leaves of 21-d-old plants grown in hydroponic conditions, essentially as described by Javot et al. (2003). Plant materials were transferred into a prefixation buffer (1.5% formaldehyde, 0.05% Triton X-100, and 50 mM phosphate buffer, pH 7.0) for 30 min at room temperature under vacuum and rinsed three times in 50 mM phosphate buffer, pH 7.0. Tissue staining was allowed to proceed by incubation in a revelation buffer (0.5 mM potassium ferricyanure, 0.5 mM potassium ferrocyanure, 1 mM 5-bromo-4-chloro-3-indolyl-GlcUA [Euromedex], and 50 mM phosphate buffer, pH 7.0) at 37°C overnight. Samples were then washed for 5 min at room temperature with 50 mM phosphate buffer, pH 7.0, and at 4°C for 2 h, in a fixation buffer (2% paraformaldehyde, 0.5% glutaraldehyde, and 100 mM phosphate buffer, pH 7.0). Plant and shoot tissues were dehydrated and/or cleared of chlorophyll by incubation in increasing (70%–100%) ethanol concentrations. For additional cross sections, roots and leaves were treated and observed as described (Javot et al., 2003).

DNA Extraction

DNA was extracted by a simplified cetyl-trimethyl-ammonium bromide method essentially as described (Javot et al., 2003). Plant material was ground in liquid nitrogen within a 1.5 mL microcentrifuge tube or alternatively in a bead blender after liquid nitrogen freezing. Each sample was then incubated in 500 μL of extraction buffer (1.4 M NaCl, 20 mM EDTA, 2% [w/v] cetyl-trimethyl-ammonium bromide, 100 mM Tris-HCl, pH 8.0, and 0.4% β-mercaptoethanol added extemporarily). After 30 min at 65°C, each sample was chloroform extracted, and DNA was precipitated twice with isopropanol and finally washed with 70% ethanol, air-dried, and dissolved in 100 μL water. Five microliters of DNA were used for each PCR reaction.

Real-Time RT-PCR

Pairs of primers for gene-specific amplification were designed in the 3′-untranslated transcribed regions of the each of 13 *AtPIP* cDNAs using PRIMER3 software (http://biotools.umassmed.edu/bioapps/primer3_www.cgi). Their sequences are displayed in Table III. RNA was extracted from leaves of plants grown under light or extended darkness conditions using a SV-RNA isolation kit (Promega) and treated by RQ1 DNAse (1 unit mg^{-1} RNA) for 1 h at 37°C. cDNAs were obtained as described above and diluted twice before any further reaction. Real-time quantification of leaf RNA was performed using a Light Cycler II (Roche). Individual PCR reaction mixtures contained 1 μL of diluted cDNA, 2 μL of reaction mix (LC Fast startDNA Master Sybr green mix; Roche), and 10 μM forward and reverse primers in 10 μL. Amplification was performed under the following conditions: 15 min at 95°C, followed by 40 cycles with 5 s at 95°, 8 s at 62°C, 10 s at 72°C, and temperature transitions of 20°C/s. Finally, a melting curve (consisting of 1 s at 95°C, 30 s at 62°C, and heating at 94°C at a rate of 0.1°C s^{-1}) was determined to ensure amplification specificity. The absence of contaminating gDNA in the cDNA template was checked by running an RT-PCR (45 cycles with an annealing temperature of 52°C) with primers specific for the *APT1* gene (At1g27450.1; 5′-CGC-CTTCTTCTCGACACTGAG-3′ and 5′-CAGGTAGCTTCTTGGGCTTC-3′). The two primers allow different size amplifications from cDNA (180 bp) and gDNA (320 bp). Data were analyzed using the Roche Lightcycler software. Cycle threshold (Ct) values were determined by the fit point method from the exponential phase of each amplification. For each gene of interest, PCR efficiency (E) was deduced from a standard dilution series, by the relation $E = -1/\text{slope}$. Relative quantification was determined using the Delta Delta Ct method with E correction and calibration with respect to one experimental condition (light conditions of experiment 2). Overall, a mean Ct value was calculated from three independent biological experiments (plant cultures), each with two PCR replicates. For normalization, four reference genes (*TIP41 like*, At4g34270; *YLS8*, At5g08290; *GAPC2*, At1g13440; and *PEX4*, At5g25760) were selected on the basis of their expression stability in leaves under light and dark conditions (Czechowski et al., 2005). Using geNORM v3.4 software (Vandesompele et al., 2002), the three more stable genes (*YLS8*, *GAPC2*, and *PEX4*) were selected, and a coefficient of variation was derived for data normalization.

Measurements of Root Osmotic Hydraulic Conductivity

Measurements were performed as described by Javot et al. (2003). Briefly, entire root systems of detopped plants were incubated in a culture medium supplemented with 10 mM Glc. After 60 min that allowed spontaneous exudation to reach a steady state level, exuded sap was collected into a graduated glass micropipette, and flow rate (J_v) was measured over the next 60 min. The osmolalities of bath medium (Π_s) and sap exuded from individual plants (Π_b) were measured by freezing-point depression osmometry. The apparent root osmotic hydraulic conductivity ($Lp_{r\text{-}o}$; in mL g^{-1} h^{-1} MPa^{-1}) was deduced from the following equation: $Lp_{r\text{-}o} = J_v/[m_r \times (\Pi_b - \Pi_s)]$, where m_r is the overall root dry mass.

Measurement of Root Hydrostatic Hydraulic Conductivity

Measurements were performed essentially as described by Javot et al. (2003) and Boursiac et al. (2005). Briefly, the root system of a freshly detopped plant was inserted into a pressure chamber filled with a PC solution containing 5 mM KNO_3, 2 mM $MgSO_4$, 1 mM $Ca(NO_3)_2$, and 10 mM MES, pH 6.0, adjusted with KOH. Pressure was then slowly applied to the chamber, and the rate of exuded sap flow (J_v) collected from the sectioned hypocotyl was determined for stabilized hydrostatic pressures (P) between 0.16 and 0.32 MPa. The root DW was determined at the end of the measurement series. The hydrostatic hydraulic conductivity of an individual root system ($Lp_{r\text{-}h}$; in mL g^{-1} h^{-1} MPa^{-1}) was calculated from the slope of a plot J_v versus P, divided by the DW of the root system.

Measurement of the Hydrostatic Rosette Hydraulic Conductivity

The entire root system of a hydroponically grown plant was excised by section at the basis of the hypocotyl. The hypocotyl was threaded into a plastic tube, and water tightness was obtained by injection within the tube of low-viscosity dental paste (President Light; Coltene) to embed the hypocotyl upper part and rosette basis. The rosette was then inserted into a pressure chamber filled with a PC solution, the plastic tube being adjusted through the soft plastic washer of the metal lid, and connected to a graduated glass micropipette. Pressure (P) was then slowly applied to the chamber using nitrogen gas. This maneuver resulted in a flow of liquid (J_v) entering through the leaf surface and exiting from the hypocotyl section. In preliminary measurements performed on about 40 rosettes, the $J_v(P)$ relationship determined for $0.1 < P < 0.7$ MPa indicated a linear relationship with an intercept of the x axis at approximately 0 MPa. The pressure tightness of the rosette-hypocotyl continuum after insertion in the pressure chamber device was established by showing that addition in the bathing solution of 0.078 g PEG6000/g water, corresponding to a 0.1 MPa osmotic pressure, resulted in similar shift of the $J_v(P)$ curve toward higher P. In routine measurements, J_v was determined over successive 10- to 20-min periods for at least three stabilized P values between 0.16 and 0.32 MPa. At the end of the measurement series, the rosette was removed, leaves were excised and scanned, and their surface area was measured using image analysis software (Optimas-Bioscan V.6-1) to determine the overall rosette surface area (S_{ros}). The hydraulic hydrostatic conductivity of an individual rosette (K_{ros}; $\mu L\ s^{-1}\ m^{-2}\ MPa^{-1}$) was calculated from the following equation: $K_{ros} = J_v/[S_{ros} \times P]$.

Effects of aquaporin inhibitors were determined at a constant pressure of 0.32 MPa by monitoring the time-dependent changes of J_v following addition of the inhibitor into the rosette bathing solution.

Protoplast Preparation and Measurement of Water Permeability (P_f)

Mesophyll protoplasts were prepared as described (Ramahaleo et al., 1999; Martre et al., 2002) by incubating leaf tissues in solution A (0.57 M sorbitol, 0.5 mM $CaCl_2$, 0.5 mM $MgCl_2$, 0.5 mM ascorbic acid, and 5 mM MES, pH 5.5) complemented with 1.5% cellulase RS and 0.25% pectolyase Y23. Isolated protoplasts were resuspended in solution A, and swelling measurements were performed at 20°C by transfer of individual protoplasts into a hypotonic solution (solution A but with 0.37 M sorbitol instead of 0.57 M sorbitol) using the procedures described by Ramahaleo et al. (1999).

Supplemental Data

The following materials are available in the online version of this article.

Supplemental Figure S1. Hydrostatic hydraulic conductivity of whole rosettes or of rosettes with all leaf blades excised.

ACKNOWLEDGMENTS

We are grateful to Gaëlle Viennois for help in GUS histochemical analyses, to Lionel Verdoucq for discussions, and to Birgit Geist for excellent technical assistance.

Received July 24, 2009; accepted December 21, 2009; published December 24, 2009.

LITERATURE CITED

Aasamaa K, Sober A (2005) Seasonal courses of maximum hydraulic conductance in shoots of six temperate deciduous tree species. Funct Plant Biol **32:** 1077–1087

Aharon R, Shahak Y, Wininger S, Bendov R, Kapulnik Y, Galili G (2003) Overexpression of a plasma membrane aquaporin in transgenic tobacco improves plant vigor under favorable growth conditions but not under drought or salt stress. Plant Cell **15:** 439–447

Alexandersson E, Fraysse L, Sjovall-Larsen S, Gustavsson S, Fellert M, Karlsson M, Johanson U, Kjellbom P (2005) Whole gene family expression and drought stress regulation of aquaporins. Plant Mol Biol **59:** 469–484

Alonso JM, Stepanova AN, Leisse TJ, Kim CJ, Chen H, Shinn P, Stevenson DK, Zimmerman J, Barajas P, Cheuk R, et al (2003) Genome-wide insertional mutagenesis of *Arabidopsis thaliana*. Science **301:** 653–657

Bläsing OE, Gibon Y, Günther M, Höhne M, Morcuende R, Osuna D, Thimm O, Usadel B, Scheible WR, Stitt M (2005) Sugars and circadian regulation make major contributions to the global regulation of diurnal gene expression in *Arabidopsis*. Plant Cell **17:** 3257–3281

Boursiac Y, Chen S, Luu DT, Sorieul M, van den Dries N, Maurel C (2005) Early effects of salinity on water transport in Arabidopsis roots. Molecular and cellular features of aquaporin expression. Plant Physiol **139:** 790–805

Bramley H, Turner NC, Turner DW, Tyerman SD (2009) Roles of morphology, anatomy, and aquaporins in determining contrasting hydraulic behavior of roots. Plant Physiol **150:** 348–364

Brodribb TJ, Holbrook NM (2004) Diurnal depression of leaf hydraulic conductance in a tropical tree species. Plant Cell Environ **27:** 820–827

Clough SJ, Bent AF (1998) Floral dip: a simplified method for *Agrobacterium*-mediated transformation of *Arabidopsis thaliana*. Plant J **16:** 735–743

Cochard H, Venisse JS, Barigah TS, Brunel N, Herbette S, Guilliot A, Tyree MT, Sakr S (2007) New insights into the understanding of variable hydraulic conductances in leaves. Evidence for a possible implication of plasma membrane aquaporins. Plant Physiol **143:** 122–133

Czechowski T, Stitt M, Altmann T, Udvardi MK, Scheible WR (2005) Genome-wide identification and testing of superior reference genes for transcript normalization in Arabidopsis. Plant Physiol **139:** 5–17

Ehlert C, Maurel C, Tardieu F, Simonneau T (2009) Aquaporin-mediated reduction in maize root hydraulic conductivity impacts cell turgor and leaf elongation even without changing transpiration. Plant Physiol **150:** 1093–1104

Fetter K, Van Wilder V, Moshelion M, Chaumont F (2004) Interactions between plasma membrane aquaporins modulate their water channel activity. Plant Cell **16:** 215–228

Flexas J, Ribas-Carbo M, Hanson DT, Bota J, Otto B, Cifre J, McDowell N, Medrano H, Kaldenhoff R (2006) Tobacco aquaporin *Nt*AQP1 is involved in mesophyll conductance to CO_2 *in vivo*. Plant J **48:** 427–439

Frangne N, Maeshima M, Schaffner AR, Mandel T, Martinoia E, Bonnemain JL (2001) Expression and distribution of a vaculoar aquaporin in young and mature leaf tissues of *Brassica napus* in relation to water fluxes. Planta **212:** 270–278

Hachez C, Heinen RB, Draye X, Chaumont F (2008) The expression pattern of plasma membrane aquaporins in maize leaf highlights their role in hydraulic regulation. Plant Mol Biol **68:** 337–353

Heinen RB, Ye Q, Chaumont F (2009) Role of aquaporins in leaf physiology. J Exp Bot **60:** 2971–2985

Hellens RP, Edwards EA, Leyland NR, Bean S, Mullineaux PM (2000) pGreen: a versatile and flexible binary Ti vector for *Agrobacterium*-mediated plant transformation. Plant Mol Biol **42:** 819–832

Jang JY, Kim DG, Kim YO, Kim JS, Kang H (2004) An expression analysis of a gene family encoding plasma membrane aquaporins in response to abiotic stresses in *Arabidopsis thaliana*. Plant Mol Biol **54:** 713–725

Javot H, Lauvergeat V, Santoni V, Martin-Laurent F, Guclu J, Vinh J, Heyes J, Franck KI, Schäffner AR, Bouchez D, Maurel C (2003) Role of a single aquaporin isoform in root water uptake. Plant Cell **15:** 509–522

Kaldenhoff R, Grote K, Zhu JJ, Zimmermann U (1998) Significance of plasmalemma aquaporins for water-transport in *Arabidopsis thaliana*. Plant J **14:** 121–128

Kaldenhoff R, Kölling A, Meyers J, Karmann U, Ruppel G, Richter G (1995) The blue light-responsive *AthH2* gene of *Arabidopsis thaliana* is primarily expressed in expanding as well as in differentiating cells and encodes a putative channel protein of the plasmalemma. Plant J **7:** 87–95

Kaldenhoff R, Kolling A, Richter G (1993) A novel blue light- and abscisic acid-inducible gene of *Arabidopsis thaliana* encoding an intrinsic membrane protein. Plant Mol Biol **23:** 1187–1198

Kaldenhoff R, Ribas-Carbo M, Sans JF, Lovisolo C, Heckwolf M, Uehlein N (2008) Aquaporins and plant water balance. Plant Cell Environ **31:** 658–666

Kammerloher W, Fischer U, Piechottka GP, Schäffner AR (1994) Water channels in the plant plasma membrane cloned by immunoselection from a mammalian expression system. Plant J **6:** 187–199

Karimi M, Inze D, Depicker A (2002) GATEWAY vectors for *Agrobacterium*-mediated plant transformation. Trends Plant Sci **7:** 193–195

Kim YX, Steudle E (2007) Light and turgor affect the water permeability (aquaporins) of parenchyma cells in the midrib of leaves of *Zea mays*. J Exp Bot **58:** 4119–4129

Lee S, Zwiazek JJ, Chung GC (2008) Light-induced transpiration alters cell water relations in figleaf gourd (*Cucurbita ficifolia*) seedlings exposed to low root temperatures. Physiol Plant **133:** 354–362

Levin M, Lemcoff JH, Cohen S, Kapulnik Y (2007) Low air humidity increases leaf-specific hydraulic conductance of *Arabidopsis thaliana* (L.) Heynh (Brassicaceae). J Exp Bot **58:** 3711–3718

Maggio A, Joly RJ (1995) Effects of mercuric chloride on the hydraulic conductivity of tomato root systems. Evidence for a channel-mediated water pathway. Plant Physiol **109:** 331–335

Martre P, Morillon R, Barrieu F, North GB, Nobel PS, Chrispeels MJ (2002) Plasma membrane aquaporins play a significant role during recovery from water deficit. Plant Physiol **130:** 2101–2110

Maurel C, Verdoucq L, Luu DT, Santoni V (2008) Plant aquaporins: membrane channels with multiple integrated functions. Annu Rev Plant Biol **59:** 595–624

Morillon R, Chrispeels MJ (2001) The role of ABA and the transpiration stream in the regulation of the osmotic water permeability of leaf cells. Proc Natl Acad Sci USA **98:** 14138–14143

Nardini A, Salleo S (2005) Water stress-induced modifications of leaf hydraulic architecture in sunflower: co-ordination with gas exchange. J Exp Bot **56:** 3093–3101

Nardini A, Salleo S, Andri S (2005) Circadian regulation of leaf hydraulic conductance in sunflower (*Helianthus annuus* L. cv Margot). Plant Cell Environ **28:** 750–759

Parent B, Hachez C, Redondo E, Simonneau T, Chaumont F, Tardieu F (2009) Drought and abscisic acid effects on aquaporin content translate into changes in hydraulic conductivity and leaf growth rate: a trans-scale approach. Plant Physiol **149:** 2000–2012

Ramahaleo T, Morillon R, Alexandre J, Lassalles JP (1999) Osmotic water permeability of isolated protoplasts. Modifications during development. Plant Physiol **119:** 885–896

Sack L, Holbrook NM (2006) Leaf hydraulics. Annu Rev Plant Biol **57:** 361–381

Sack L, Melcher PJ, Zwieniecki MA, Holbrook NM (2002) The hydraulic conductance of the angiosperm leaf lamina: a comparison of three measurement methods. J Exp Bot **53:** 2177–2184

Sakurai J, Ahamed A, Murai M, Maeshima M, Uemura M (2008) Tissue and cell-specific localization of rice aquaporins and their water transport activities. Plant Cell Physiol **49:** 30–39

Santoni V, Vinh J, Pflieger D, Sommerer N, Maurel C (2003) A proteomic study reveals novel insights into the diversity of aquaporin forms expressed in the plasma membrane of plant roots. Biochem J **372:** 289–296

Schardl CL, Byrd AD, Benzion G, Altschuler MA, Hildebrand DF, Hunt AG (1987) Design and construction of a versatile system for the expression of foreign genes in plants. Gene **31:** 1–11

Siefritz F, Tyree MT, Lovisolo C, Schubert A, Kaldenhoff R (2002) PIP1 plasma membrane aquaporins in tobacco: from cellular effects to function in plants. Plant Cell **14:** 869–876

Smith SM, Fulton DC, Chia T, Thorneycroft D, Chapple A, Dunstan H, Hylton C, Zeeman SC, Smith AM (2004) Diurnal changes in the transcriptome encoding enzymes of starch metabolism provide evidence for both transcriptional and posttranscriptional regulation of starch metabolism in Arabidopsis leaves. Plant Physiol **136:** 2687–2699

Steudle E, Peterson CA (1998) How does water get through roots? J Exp Bot **49:** 775–788

Suga S, Maeshima M (2004) Water channel activity of radish plasma membrane aquaporins heterologously expressed in yeast and their modification by site-directed mutagenesis. Plant Cell Physiol **45:** 823–830

Tournaire-Roux C, Sutka M, Javot H, Gout E, Gerbeau P, Luu DT, Bligny R, Maurel C (2003) Cytosolic pH regulates root water transport during anoxic stress through gating of aquaporins. Nature **425:** 393–397

Tyree MT, Nardini A, Salleo S, Sack L, El Omari B (2005) The dependence of leaf hydraulic conductance on irradiance during HPFM measurements: any role for stomatal response? J Exp Bot **56:** 737–744

Uehlein N, Otto B, Hanson DT, Fischer M, McDowell N, Kaldenhoff R (2008) Function of *Nicotiana tabacum* aquaporins as chloroplast gas pores challenges the concept of membrane CO_2 permeability. Plant Cell **20:** 648–657

Vandesompele J, De Preter K, Pattyn F, Poppe B, Van Roy N, De Paepe A, Speleman F (2002) Accurate normalization of real-time quantitative RT-PCR data by geometric averaging of multiple internal control genes. Genome Biol **3:** RESEARCH0034

Wiese A, Christ MM, Virnich O, Schurr U, Walter A (2007) Spatio-temporal leaf growth patterns of *Arabidopsis thaliana* and evidence for sugar control of the diel leaf growth cycle. New Phytol **174:** 752–761

Ye Q, Holbrook NM, Zwieniecki MA (2008) Cell-to-cell pathway dominates xylem-epidermis hydraulic connection in *Tradescantia fluminensis* (Vell. Conc.) leaves. Planta **227:** 11311–11319

Zelazny E, Borst JW, Muylaert M, Batoko H, Hemminga MA, Chaumont F (2007) FRET imaging in living maize cells reveals that plasma membrane aquaporins interact to regulate their subcellular localization. Proc Natl Acad Sci USA **104:** 12359–12364